Determination of the vaporization order of crude oils through the chemical analysis of crude oil residues burned on water

Chemosphere 285 (2021) 131563

Contents lists available at ScienceDirect

Chemosphere

journal homepage: www.elsevier.com/locate/chemosphere

Determination of the vaporization order of crude oils through the chemical analysis of crude oil residues burned on water

Laurens Van Gelderen [a,1,*], Kristoffer Gulmark Poulsen [b], Jan H. Christensen [b], Grunde Jomaas [a,c]

[a] Department of Civil Engineering, Technical University of Denmark, Kgs., Lyngby, Denmark
[b] Department of Plant and Environmental Sciences, Thorvaldsensvej 40, University of Copenhagen, 1871, Frederiksberg C, Denmark
[c] School of Engineering, BRE Centre for Fire Safety Engineering, University of Edinburgh, Edinburgh, United Kingdom

ARTICLE INFO

Handling Editor: Y Yeomin Yoon

Keywords:
Oil spill response method
In-situ burning
Burning efficiency
Polycyclic aromatic
Hydrocarbons
Environmental benefit analysis

ABSTRACT

To determine the vaporization order of (the components in) crude oils, the density, the viscosity and the chemical composition of a light and a heavy crude oil were studied as a function of the burning efficiency. An experimental series of small scale in-situ crude oil burns on water were conducted with the two crude oils. Chemical analyses of the burned residues showed that the components in crude oils vaporize in order of decreasing volatility and the depletion rate of components generally decreased with increasing molecular mass. Ultimately, this means that the burning efficiency of a crude oil burning on water can be related to fire dynamics principles, irrespective of its chemical and physical properties. The relative abundance of pyrogenic PAHs in the burned residues increased up to a maximum of 2600% for the light crude oil and 9100% for the heavy crude oil. Increased abundances of the pyrogenic PAHs were caused by the formation of the pyrogenic PAHs during the burning and not by an increase in concentration in the burned residues. Overall, the results provide relevant data for predicting the effectiveness of in-situ burning of crude oil as oil spill response method, both in terms of its burning efficiency and its environmental impact.

1. Introduction

In-situ burning of spilled oil is one of the main oil spill response methods. This method removes oil from the water surface by turning the oil into soot and other (gaseous) combustion products (Buist et al., 1999, 2013; Potter and Buist, 2008; Fingas, 2011). The two best known examples of the in-situ burning of accidently spilled oil are from the *Exxon Valdez* spill (Allen, 1990) and the *Deepwater Horizon* spill (Allen et al., 2011). For the *Exxon Valdez* spill, an estimated burning efficiency of 98–99%, in weight percentage of oil removed from the water surface, was reported. Achieving such a high burning efficiency (>90%) is very important because the burning efficiency is the primary aspect of in-situ burning that determines its effectiveness as oil spill response method. The properties that determine whether an in-situ burn of crude oil on water will acquire the desired burning efficiency are, however, not well understood.

One such property is the vaporization order of crude oils, which determines the order in which the thousands of hydrocarbons of a crude oil evaporate from the oil to participate in an (in-situ) fire. The fire properties of hydrocarbons, such as the heat of combustion and the heat of vaporization, are a function of their molecular structures (Egloff et al., 1940; Prosen and Rossini, 1945; Bradford and Thodos, 1967; Vetere, 1979; Seaton and Keith Harrison, 1990; Růžička and Majer, 1994; Nolan, 2011). As such, the vaporization order governs, at every stage of the fire, the heat that is released and the heat that is needed to maintain a sufficient evaporation rate that can sustain the fire. Once the fire can no longer generate sufficient heat to sustain the fire, e.g. due to heat losses or insufficient fuel, the fire will extinguish and any remaining crude oil is left as a burned residue on the water surface. This means that the vaporization order of a crude oil partly determines when an in-situ burning fire will extinguish and thereby its burning efficiency. Understanding the vaporization order is therefore important when trying to predict the effectiveness of in-situ burning as oil spill response.

Currently, conflicting theories have been published on the vaporization order of multicomponent fuels, from which two main hypotheses can be derived. The first hypothesis states that burning crude oils act like

* Corresponding author.
E-mail address: lpvg@outlook.com (L. Van Gelderen).
[1] *Present address: Netherlands Forensic Institute, Laan van Ypenburg 6,* 2497 GB, *the Hague, the Netherlands.*

https://doi.org/10.1016/j.chemosphere.2021.131563
Received 3 May 2021; Received in revised form 10 July 2021; Accepted 13 July 2021
Available online 15 July 2021

pure fuels, with all components evaporating simultaneously, each at a constant rate (equilibrium flash vaporization) (Petty, 1983; Buist et al., 2013). Depending on the evaporation rates of the component and their respective concentrations in the crude oil, the chemical composition of the oil may or may not change as the fire progresses (Buist et al., 1997). The second hypothesis states that the components in multicomponent fuels evaporate in order of decreasing volatility, with evaporation rates of the components changing accordingly (diffusion-limited vaporization) (Law, 1978, 2006; Wang et al., 1984). Starting with the highest volatility, components with similar volatilities evaporate simultaneously until their concentrations in the fuel are too low to provide the burning rate required to sustain the fire. Less volatile components then start evaporating to feed sufficient combustible gases to the fire, while the more volatile components are being fully depleted from the fuel. This process continues until all components are depleted from the fuel or until the heat generated by the remaining components can no longer generate a sufficient evaporation rate. During in-situ burning, the composition of the components participating in the fire and the composition of the crude oil would thus constantly change as the fire progresses. Fundamentally, the two hypotheses are very different and presently conclusive evidence has not been provided for either hypothesis.

In a previous study (Van Gelderen et al., 2017), we showed through small scale experiments that the diffusion-limited vaporization model could best explain the observed fire behavior of crude oil burning on water. This conclusion was, however, derived from indirect (physical) measurements of the flames and the burning oil. The study also included a chemical analysis of the fresh crude oil and of a burned residue, but only after the fire naturally extinguished. Analysis of the chemical composition of a burning crude oil as a function of the burning progression would provide more conclusive data on which vaporization order is followed by burning crude oils. In this study, burned crude oil residues from different stages of in-situ fires were therefore sampled and analyzed using gas chromatography and mass spectrometry to determine their chemical compositions. The vaporization order of the crude oils was then determined from the observed changes in the chemical composition of the burned residues as a function of the burning progression.

Analyzing the chemical composition of burned residues is also relevant from an environmental perspective. For example, in a recent review on residues from the in-situ burning of oil spills, Fritt-Rasmussen et al. (2015) showed that there are still many unanswered questions regarding the formation, fate and environmental impact of burned residues. Among others, heavy polycyclic aromatic hydrocarbons (PAHs) are known to increase in concentration in burned crude oil residues. These PAHs "have a higher potential for bioaccumulation and, in addition, may include mutagens and carcinogens such as benzo[a]pyrene" (Fritt-Rasmussen et al., 2015, p. 9). Stout and Payne (2016) showed qualitatively, through comparison of heavy PAH concentrations in burned residues, that heavy PAH concentration increases had to be due to formation of these PAHs during combustion. The current study provides complementing quantitative data on which heavy PAHs are formed during in-situ burning, independent of the changes in other components in the crude oils. The results presented herein thus also support assessments of the environmental impact of in-situ burning by providing quantitative data on the removal and the formation of analyzed PAHs.

2. Materials and methods

2.1. In-situ burning setup

The burning experiments were conducted in a modified version of the previously used Crude Oil Flammability Apparatus (COFA) (Van Gelderen et al., 2015). The modified COFA setup features a short Pyrex glass cylinder with a height of 50 mm and an inner diameter of 163 mm, placed on a metal stand in the middle of a water basin of 1.0 × 1.0 × 0.50 m^3 (Fig. 1). A propeller is fixed on the middle of one of the walls of the basin and is used to create a current in the water body. On the water surface inside the Pyrex glass cylinder, the crude oil is contained and burned. Because of the low height of the cylinder compared to the original COFA setup, the water layer below the burning oil can be continuously refreshed, and thus cooled, by the current in the water body. This is a significant modification from the original COFA setup, in which the water layer below the burning oil would superheat, ultimately causing a boilover (Arai et al., 1990; Garo et al., 1994). A boilover is an explosive burning state that, once initiated, rapidly extinguishes fire. This phenomenon is typically not observed during in-situ burning operations on sea (Buist et al., 2013) and is mostly an artifact of laboratory experiments. The modified COFA setup is thus more representative of full scale in-situ burning operations than the original COFA setup.

In order to determine whether the proposed vaporization order theory is applicable to any crude oil, a light crude oil from the Danish Underground Consortium (DUC) and a heavy crude oil from the Grane oil field were studied. For the same purpose, DUC crude oil was tested for initial slick thicknesses of 5 and 20 mm. Because of supply limitations, Grane crude oil was only tested for an initial slick thickness of 5 mm. The relevant chemical and physical properties of these crude oils are shown in Table 1. More detailed information on the hydrocarbon fractions of the two crude oils is included in the Supplementary Materials.

Prior to conducting the experimental series, the flow velocity of the propeller and its vertical distance to the Pyrex glass cylinder were optimized. The flow in the water body of the COFA has to cool the water layer below the burning oil sufficiently in order to prevent boilover, but should at the same time not cause disturbances at the fuel surface. The initial location of the propeller was chosen to result in minimally observable waves on the water surface opposite of the cylinder. Then, starting with a 5 mm thick DUC slick, an experiment was run where the oil either burned until natural extinction or until boilover. If the fire ended in a boilover, the experiment was repeated with a higher flow velocity or with the propeller closer to the cylinder. If the fire extinguished naturally, the time was noted until extinction and the residue was sampled and collected as described above. This process was repeated for a 20 mm thick DUC slick and a 5 mm thick Grane slick, each starting with the propeller setup of the previously tested oil type. For reference, in this study the propeller was located approximately 20 cm below the Pyrex glass cylinder and had a flow velocity of 1000 L/h for DUC and 2500 L/h for Grane. Grane, being heavier than DUC, burns at higher temperatures and thus the water layer below the burning Grane requires more cooling through a higher propeller velocity to prevent boilover from occurring.

2.2. In-situ burning experimental procedure

For each crude oil (5 mm DUC, 20 mm DUC and 5 mm Grane), it was aimed to obtain burned residue samples as a function of the burning progression in burning efficiency intervals of 10% (i.e. 10%, 20%, 30%, etc.), up until their maximum burning efficiency. Monitoring the burning efficiency during a fire and taking residue samples from a burning crude oil are, however, practically unfeasible. Every burned residue sample with a specific burning efficiency therefore required its own experiment. As such, multiple experiments had to be conducted for each oil, with the experiments being manually extinguished at different burning times that corresponded with the required burning efficiency. The maximum burning efficiency for each crude oil, for the used experimental setup, was obtained by letting the fire extinguish naturally. The exact correlation between the burning time and the burning efficiency was not known prior to conducting the experimental series though and had to be determined as the series was conducted. The methodology for this process is explained in the Supplementary Materials.

In a typical experiment, the COFA was filled with water until the

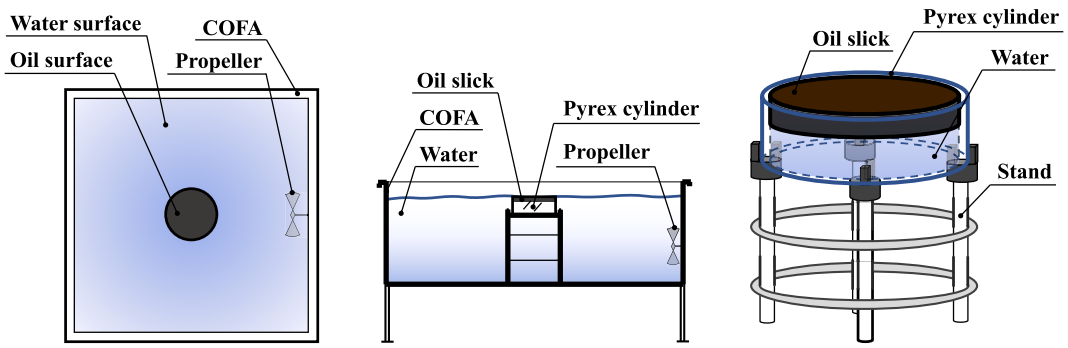

Fig. 1. Schematic of the modified COFA setup, adapted and modified from Van Gelderen and Jomaas (2018).

Table 1
Physical and chemical characteristics of DUC and Grane.

Oil	*Density (g/ml)*[a]	*Boiling point (°C)*	*Flashpoint (°C)*[b]	*Viscosity (cP)*[a]	*Wax content (wt %)*	*Asphaltenic content (wt %)*	*Total sulfur (wt %)*	*Vanadium (ppm)*	*Nickel (ppm)*
DUC	0.853	≥230	7	6.750	4.2[c]	<0.05[c]	0.261[c]	<1[c]	6[c]
Grane	0.934	≥380	20–21	268.7	7.0[d]	0.9[d]	0.62[d]	9.5[d]	3.1[d]

[a] Measured at 25 °C using an Anton Paar SVM 3000 viscometer.
[b] Measured using a Pensky-Martens Flash Point Tester: PM 4 (closed cup).
[c] Maersk Maersk Oil, 2005.
[d] Statoil (2017), different values have been reported for the wax and asphaltenic content in Fritt-Rasmussen et al. (2012).

water level was approximately 10–30 mm below the Pyrex cylinder edge. A known quantity of crude oil (m_{oil}), corresponding to a slick thickness of 5 or 20 mm, was then carefully poured onto the water surface inside the Pyrex glass cylinder. Care was taken during the pouring process that any resurfacing oil would not resurface outside of the cylinder. Additional water was then slowly added to the basin until the oil surface was 1–2 mm below the edge of the cylinder. The temperature of the water body was measured to be able to assess the influence, if any, of the initial water temperature on the burning efficiency. Then, the propeller was turned on and the oil was ignited using a butane torch blower, at which point a stopwatch was started.

After the estimated amount of time (see the Supplementary Materials), the fire was extinguished by placing a non-combustible cover over the Pyrex glass cylinder. A 3–5 ml sample was taken from the surface of the burned residue with a pre-weighed syringe for measurements of the viscosity and density of the residue. Care was taken that no water from below the residue was sampled. If needed, any collected water in the syringe was ejected and additional residue was sampled with the syringe so that it contained at least 3 ml of burned residue. The residue in the syringe was then weighed (m_{visc}) and injected in the viscometer. Next, a 1–2 ml sample of the residue was collected with a spatula and stored in a pre-weighed glass vial. The residue in the vial was weighed (m_{vial}) and stored in a freezer prior to the chemical analysis (see below). The remaining residue was collected with pre-weighed hydrophobic absorption pads and weighed (m_{res}), so that the burning efficiency could be determined using Eq. (1). Grane residues were dried overnight to evaporate any water taken up by the residue as Grane has a high affinity for water because of its high asphalthenic content.

$$Burning\ efficiency = \left(1 - \frac{m_{visc} + m_{vial} + m_{res}}{m_{oil}}\right) \cdot 100\% \quad (1)$$

2.3. Chemical analysis

The residues samples (43 in total) were diluted in dichloromethane (DCM, HPLC grade – Rathburn, UK) to concentrations of 1–2 mg/ml. The samples were analyzed with an Agilent 6890 N/5975 gas chromatograph – mass spectrometer (GC – MS) operating in electron ionisation (EI) mode. The GC was equipped with a 60 m ZB-5 (0.25 mm inner diameter, 0.25 μm film thickness) capillary column (Phenomenex, USA). Helium was used as carrier gas with a flow rate of 1.1 mL/min. Aliquots of 1 μL were injected in pulsed splitless mode with an inlet temperature of 315 °C. The column temperature program was as follows: an initial temperature of 40 °C held for 2 min, then a 25 °C min^{-1} increase to 100 °C followed by an increase of 5 °C min^{-1} to 315 °C, which then was held for 13.4 min resulting in a total run time of 60.8 min. The transfer line, ion source and quadrupole temperatures were 315 °C, 230 °C and 150 °C, respectively. A total of 55 mass-to-charge ratios (m/z) were acquired in SIM mode. The complete description of the GC-MS/SIM method can be found in (Gallotta and Christensen, 2012). A Quality Control (QC) sample, representative of the sample matrix, was constructed by taking equal amounts of half of the DUC residue samples to measure instrumental variability. The residue samples were split into two analytical batches. These batches included five QC sample replicates and six solvent blanks (DCM), spread throughout the analytical sequence in order to monitor the analytical quality.

2.4. Data processing

Chromatographic peak integration of 67 chemical components and 26 component groups, consisting of polycyclic aromatic hydrocarbons (PAHs), *n*-alkanes and petroleum biomarkers, was performed using Masshunter Workstation Software – Quantitative Analysis (Version B.07.00). The selected ion chromatograms were integrated according to the CEN/TR 15522-2 (2012) protocol in order to include only the relevant peaks and peak regions of interest. The integration data (peak area) were then exported as a.csv file into Excel where the data were processed as described below. A complete overview of the 93 analyzed components and component groups is shown in the Supplementary Materials.

The relative abundance of each component or component group in a residue sample, with respect to their corresponding fresh starting oils, was derived by a three-step normalization procedure. First, for each residue sample, its components and component groups were internally normalized using the weathering resistant 17α,21β-hopane to remove variations due to absolute concentration differences. We are aware of a study that shows C_{30}-αβ hopane not to be fully resistant to thermal degradation in burning oil (John et al., 2018). The burning experiments

in John et al. (2018) were, however, conducted under very different conditions than in-situ burning experiments in general and as conducted in this study. They diluted the crude oil in hexane and dichloromethane and burned the crude oil 16 times, igniting the residues again with hexane, which could have caused the degradation of the C_{30}-αβ hopane. We therefore considered 17α,21β-hopane to still be the most viable component for internal standardization for this study. Next, each component and each component group was normalized to a QC normalization factor (QC_{norm}) (Eq. (2)). This step reduces the systematic discrimination throughout and between the analytical sequences.

$$QC_{norm,C_{n,r}} = \frac{\frac{C_{n,QC_r}}{\alpha,\beta-H_{QC_r}}}{\frac{C_{n,\ QC_0}}{\alpha,\beta-H_{QC_0}}} \tag{2}$$

Here, C_n is the abundance of the nth component (group) and $\alpha,\beta-H$ is the abundance of 17α,21β-hopane. The subscripts are for the replicate QC sample nearest in the analysis sequence to the residue sample (QC_r) and the replicate QC sample nearest in the analysis sequence to the corresponding fresh crude oil (QC_0). The result is the QC normalization factor for the nth component (group) of residue sample r ($QC_{norm,C_{n,r}}$). An overview of the sampling sequence with an example calculation of the QC normalization factor is included in the Supplementary Materials.

Finally, each component (group) was normalized to its corresponding component (group) of the respective fresh oil (DUC or Grane) ($C_{n,f}$) in order to obtain the relative abundance (in %) of that component (group) in the residue sample. This process is summarized in Eq. (3). For the fresh oils, the QC normalization factor ($QC_{norm,C_{n,f}}$) equals 1 by definition, as the same replicate QC sample is used in the numerator and denominator of Eq. (2).

$$\textit{Relative abundance}\ C_{n,r} = \frac{\frac{\left(\frac{C_{n,r}}{\alpha,\beta-H_r}\right)}{QC_{norm,C_{n,r}}}}{\frac{\left(\frac{C_{n,f}}{\alpha,\beta-H_f}\right)}{QC_{norm,C_{n,f}}}} \cdot 100\% = \frac{\left(\frac{C_{n,r}}{\alpha,\beta-H_r}\right)}{\left(\frac{C_{n,f}}{\alpha,\beta-H_f}\right)} \cdot 100\% \tag{3}$$

Here, C_n is the abundance of the nth component (group) and $\alpha,\beta-H$ is the abundance of 17α,21β-hopane in the same sample, with the subscripts r for the residue sample and f for the fresh crude oil.

3. Results and discussion

3.1. In-situ burning experiments

The burning efficiencies as a function of the burning time for DUC (5 and 20 mm initial slick thickness) and Grane (5 mm initial slick thickness) are shown in Fig. 2. The results for the repetition series of DUC show that the experiments have a good repeatability, with deviations in the burning efficiencies between repetitions of 1.4–11%.[2] In both these experimental series, the burning rate (in g/s) decreased as a function of the burning time, from 0.18 to 0.096 g/s for 5 mm DUC and from 0.23 to 0.12 g/s for 20 mm DUC. This difference in burning rates with varying initial slick thicknesses is a known phenomenon for burning crude oils on water (see e.g. (Buist et al., 1999; Buist et al., 2013)). As expected, the burning rates for the lighter DUC crude oil were higher than the burning rates for the heavier Grane crude oil (0.14–0.068 g/s). A more in-depth discussion on the influence of the initial slick thickness and oil types on the burning rate and the burning efficiency is beyond the scope of this paper and has already been covered in the literature (see also (Garo et al., 1994; Garo et al., 1999; Brogaard et al., 2014; Van Gelderen et al., 2015; Van Gelderen et al., 2017)). Overall, the burning efficiency results show that the collected samples provide a good selection of data points along a reasonably predictable burning rate curve that is in accordance with previous studies. As such, these samples were deemed appropriate for studying the chemical composition of burning crude oil as a function of the burning progression.

Fig. 3 shows the measured density and dynamic viscosity as a function of the burning efficiency for DUC and Grane. Both the density and viscosity increased with increasing burning efficiency. Hydrocarbons generally show an increase in density and viscosity with decreasing volatility (Carmichael et al., 1964; Piacente et al., 1994; Korsten, 2001; Chickos and Hanshaw, 2004; Yaws, 2015) and the results thus indicate that, with decreasing volatility, crude oil components vaporize slower, at later stages of the fire, or both slower and later. The constant vaporization rate model, but only when lighter components vaporize faster than heavier components, and the diffusion-limited vaporization model both match with these results.

The results in Fig. 3 also show that there is a distinct, albeit small, difference between the results for 5 mm and 20 mm DUC. For both the density and viscosity, 5 mm and 20 mm DUC follow very similar trendlines, but the values for 20 mm DUC are consistently lower. This is caused by the 20 mm DUC residues having a slightly higher relative abundance of the lighter components than the 5 mm DUC residues at the same burning efficiency (see also Section 3.2.1 and the Supplementary Materials). Such a difference in relative abundances must be caused by either differences in the composition of the vaporizing components or their individual vaporization rates, for different initial slick thicknesses. Why these differences occurred could not be explained with the obtained results and further research into this topic was beyond the scope of this study. Ultimately, the results in Fig. 3 indicate that the vaporization order is not solely a function of the initial chemical composition of the crude oil. Physical parameters, such as the initial slick thickness, clearly have an influence as well on which components, at which rate, evaporate during which stage of the fire.

3.2. Chemical analysis of burned residues

3.2.1. n-Alkanes and isoprenoids

The results of the chemical analyses of *n*-alkanes (C_{10} to C_{32}) and isoprenoids (nor-pristane, pristane and phytane) in the 5 mm DUC burned residues are shown in Fig. 4. Because of the normalization method (Eq. (2) and (3)), each data point effectively shows the abundance of a component in a residue sample relative to the abundance of that component in the corresponding fresh oil. For example, at a burning efficiency of 47%, the relative abundance of phytane was 34%, which means that 66% of the phytane originally present in the fresh DUC has been burned. The observed relative abundance of >100% for some components is likely a result of experimental and analytical uncertainties, rather than the actual formation of these components. Overall, the results show good precision for sample pairs with similar burning efficiencies (8.1% and 9.0%, 19% and 20%, 28% and 31%, 33% and 35%, 38% and 40%, 47% and 50%, and 53% and 55%). For each sample pair, the average of the absolute differences in relative abundance per component was ≤5.6% (with a standard deviation of 3.8%). An example of this calculation for the residues with burning efficiencies of 8.1% and 9.0% is given in Eq. (4).

$$\frac{1}{N}\sum_{n=1}^{N}\left|C_{n,r1}-C_{n,r2}\right|,\ \frac{1}{26}\sum_{n=1}^{26}\left|C_{n,8.1\%}-C_{n,9.0\%}\right| = 3.2\% \tag{4}$$

The components in Fig. 4 are shown in order of increasing retention time, which is a measure for an increasing molecular mass and decreasing volatility (Piacente et al., 1994; Chickos and Hanshaw, 2004). The resulting relative abundance profiles of straight and branched alkanes provide a clear overview of the changes in the chemical composition of the residues as a function of the burning efficiency. In general, with increasing burning efficiency, the relative

[2] The two highest relative deviations were for the burning efficiencies of 9.0% and 8.1% for 5 mm DUC (11% deviation) and burning efficiencies of 40% and 37% for 20 mm DUC (9.5% deviation).

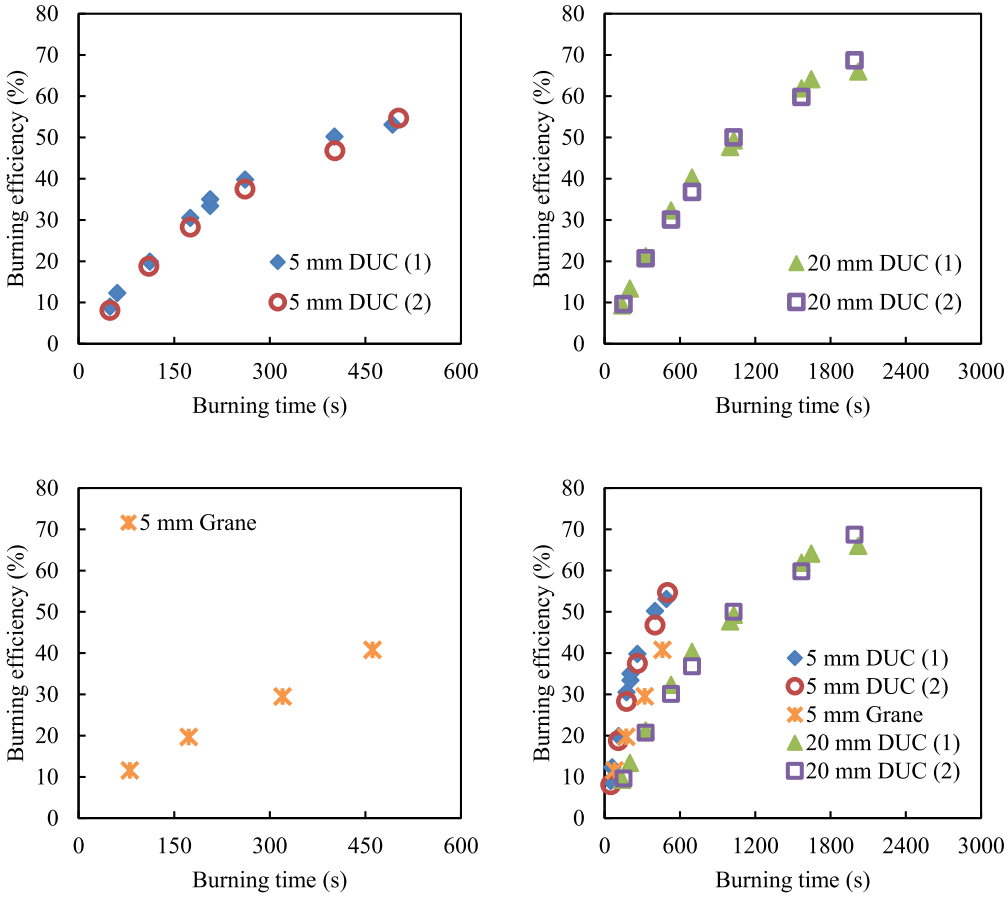

Fig. 2. Burning efficiencies as a function of the burning time for 5 mm DUC, 20 mm DUC and 5 mm Grane. The numbers in parentheses in the legends annotate the original series (1) and the repetition (2). The fourth graph shows all the data combined for comparison purposes.

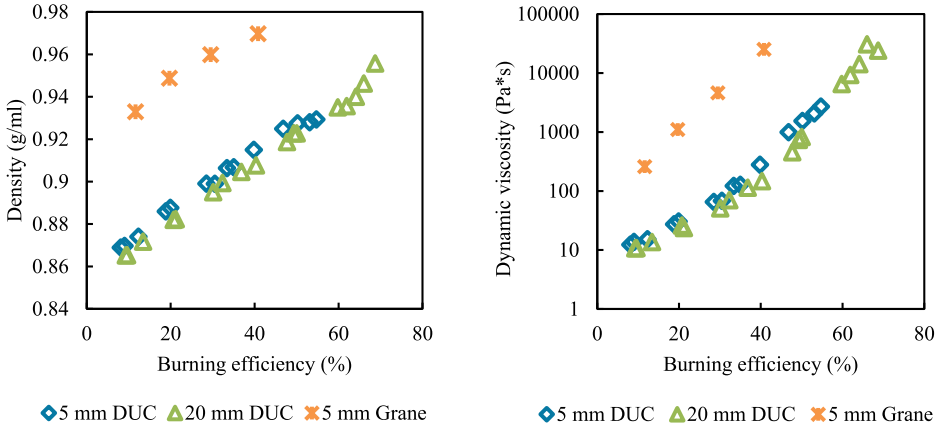

Fig. 3. Density and dynamic viscosity as a function of the burning efficiency for DUC and Grane.

abundancy of the lighter *n*-alkanes and isoprenoids (C_{10} - C_{28}) was reduced more compared to the heavier *n*-alkanes (C_{29} - C_{32}). For example, at a burning efficiency of ≥50%, C_{10} - C_{14} were almost completely removed (≤5% remaining) compared to 87–99% remaining of C_{28} - C_{32}. This correlates well with the observed increase in density and viscosity with increasing burning efficiency (Fig. 3).

More specifically, Fig. 4 show that the depletion rate from the burned residues of the components decreased with increasing molecular mass of the components. Thus, the more volatile a component, the faster it was removed from the burning oil. Furthermore, the results show that the heavier a component, the later it started to evaporate from the burning oil to participate in the fire. At a burning efficiency of 38%, which corresponds to a burning time of 260 s, the heaviest *n*-alkanes (C_{28} - C_{32}) had not started burning, still showing relative abundances of 100% to 17α,21β-hopane. In summary, multiple components were depleted simultaneously, with the exact composition of which components varying as a function of the burning time. All of these results correspond very well, and only, with the proposed diffusion-limited vaporization

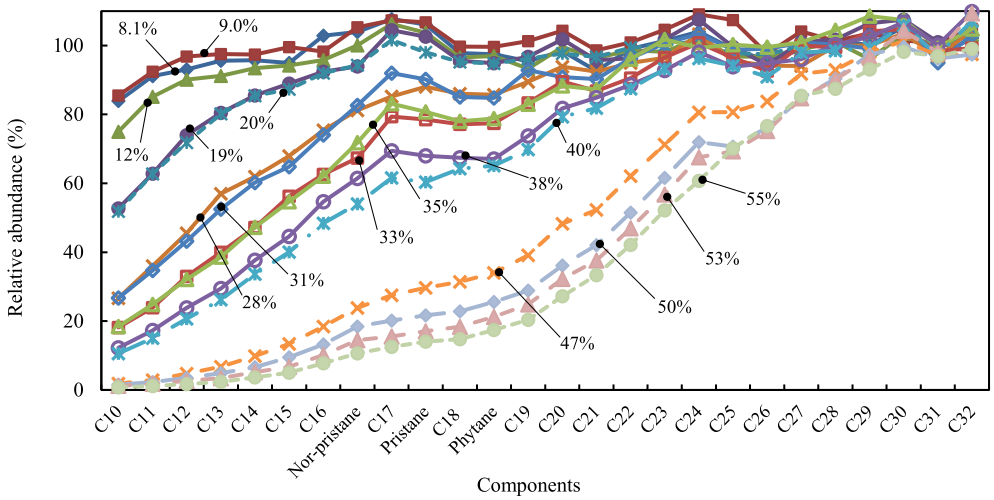

Fig. 4. Relative abundance of *n*-alkanes (C_nH_{2n+2}) and isoprenoids in burned 5 mm DUC residues as a function of the burning efficiency. The components are sorted in order of increasing retention time. The lighter and more volatile components participated in the fire earlier and were depleted faster from the burning crude oil than the heavier and less volatile components.

order and provide strong experimental evidence in support of this crude oil vaporization model.

The relative abundance results for the *n*-alkanes and isoprenoids of 20 mm DUC and 5 mm Grane (see the Supplementary Materials) correspond well with the results for 5 mm DUC and confirm the conclusion above. These matching results indicate that the general principles of the diffusion-limited vaporization model are applicable to crude oils in general, independent of their specific chemical and physical properties. The actual depletion rate of each component, however, was different for the different tested oils (5 mm DUC, 20 mm DUC and 5 mm Grane). At 50% burning efficiency, for example, icosane (C_{20}) had a relative abundance of 36% in 5 mm DUC compared to 55% in 20 mm DUC. Also in Grane, at 20% burning efficiency, the relative abundance of icosane was reduced to 57%, whereas for both 5 mm and 20 mm DUC, the icosane was not yet (measurably) being depleted. Within the diffusion-limited vaporization model, onset of vaporization and the depletion rate of each component is thus determined by the specific chemical and physical properties of a crude oil. This was also discussed in Section 3.1.

3.2.2. *Polycyclic aromatic hydrocarbons*

Fig. 5 shows the relative abundance results for petrogenic (occurring naturally in crude oil) PAHs in the 5 mm DUC residues as a function of the burning efficiency. The results for PAHs that were primarily formed during combustion, i.e. pyrogenic PAHs, are discussed below. The petrogenic PAHs data set consists of naphthalene (N), alkylated benzothiophenes (BT), fluorene (F), dibenzothiophene (DBT), phenanthrene (P), pyrene (Py), retene, chrysene (Ch) and their alkylated derivatives. For clarity reasons, the results for pyrene and methylpyrene are included with the pyrogenic PAHs results. In addition, only the component groups of the alkylated PAHs are shown. For example, component group C_1–N contains the results for both 1-methylnaphthalene and 2-methylnaphthalene. Because the results for the petrogenic and pyrogenic PAHs were functionally the same for all tested crude oils, only the results for 5

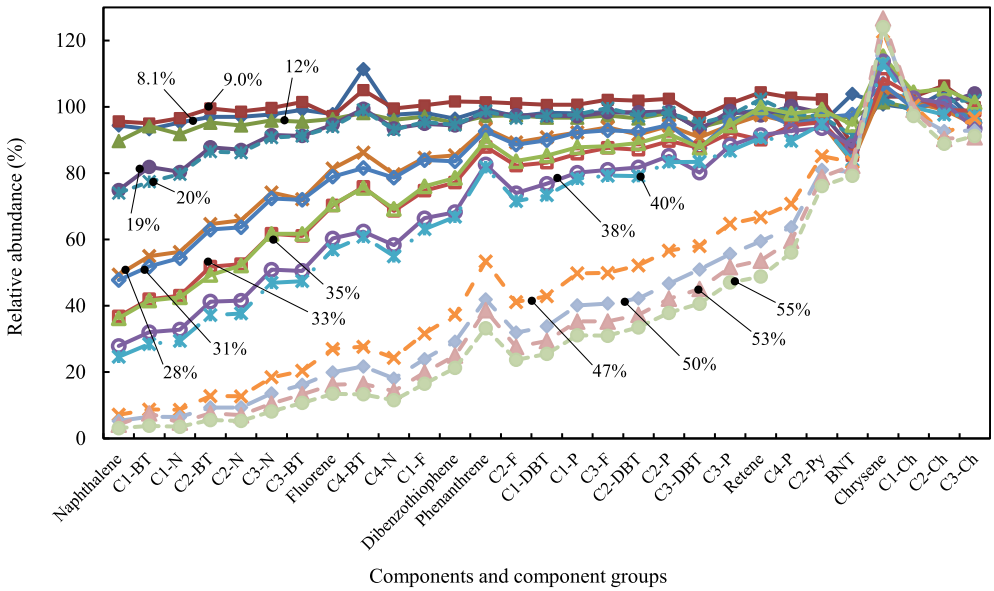

Fig. 5. Relative abundance of petrogenic PAHs in burned 5 mm DUC residues as a function of the burning efficiency. The components and component groups are sorted in order of increasing retention time. The lighter and more volatile components participated in the fire earlier and were depleted faster from the burning crude oil than the heavier and less volatile components.

mm DUC are shown here. A detailed overview with the relative abundance results for all of the analyzed alkylated PAHs, including the results for 20 mm DUC and 5 mm Grane, can be found in the Supplementary Materials. The full names of the abbreviated components and component groups are also included in the Supplementary Materials.

The results for the petrogenic PAHs, shown in order of increasing retention time, show the same trends as for the *n*-alkanes, and isoprenoids. The depletion rate of the petrogenic PAHs generally decreases with increasing molecular mass and thus with decreasing volatility. This trend was also observed for the omitted individual alkylated PAHs (as shown in the Supplementary Materials). At the highest obtained burning efficiency of 55%, the lightest alkylated naphthalenes and benzothiophenes were nearly fully removed from the residue (Fig. 5). The alkylated chrysenes, on the other hand, only just started to participate in the fire. Notably, chrysene increased in relative abundance, while it was not considered to be a pyrogenic PAH for the purposes of this study. Chrysene was possibly formed more during the fire than it was removed as fuel. Alternatively, triphenylene, which co-eluted with chrysene, may have been formed by the fire instead (see e.g. Constantinidis et al. (2015)) and thereby increased the measured relative abundance of chrysene. A detailed study in the formation of either chrysene or triphenylene during the combustion of the crude oils was, however, beyond the scope of this study. Regardless, the overall petrogenic PAH results show that the diffusion-limited vaporization order also applies to the more complex components in a crude oil.

Fig. 6 shows the relative abundance results for a selection of pyrogenic PAHs in the 5 mm DUC residues as a function of the burning efficiency. The shown pyrogenic PAHs all reached relative abundances of at least 200%. The highest relative abundances were reached for benzo[k]fluoranthene (1877%), benzo[a]pyrene (750%) and indeno(1,2,3-c,d)pyrene (1614%). These components reached relative abundances of respectively 2142%, 974% and 2570% in the 20 mm DUC residues, and 9108%, 482% and 680% in the 5 mm Grane residues. A complete overview of all analyzed pyrogenic PAH components, including the results for 20 mm DUC and 5 mm Grane, is included in the Supplementary Materials. The most notable result in Fig. 6 is that the relative abundance of acenaphthylene initially increased with increasing burning efficiency, but declines after a burning efficiency of 40% is reached. This indicates that as the burning progresses, smaller pyrogenic PAHs start to participate in the fire and shift from being mainly a combustion product to being mainly fuel for the fire.

Increased pyrogenic PAH abundances in crude oil residues are a well-known effect of burning crude oils, as shown by several other studies on in-situ burning residues (see e.g. (Fingas et al., 1994; Wang et al., 1999; Fritt-Rasmussen et al., 2013; Fritt-Rasmussen et al., 2015; Stout and Payne, 2016) and references therein). It is not always clear if such an increase in abundance is due to the formation of the pyrogenic PAHs, the depletion of other components from the burning oil, or a combination of both processes. Because of the normalization process used in this study (Eq. (3)), the depletion of the *n*-alkanes, isoprenoids and lighter PAHs does not affect the abundance of the pyrogenic PAHs. This means that the results shown in Fig. 6 are (primarily) because the quantity of the pyrogenic PAHs in the burned residues was increased. Enrichment of burned residues with pyrogenic PAHs is typically considered to be caused by precipitation of particles that are formed during the combustion reactions in the gas phase. Alternatively, pyrogenic PAHs could also be formed in the residue itself by thermal conversion reactions when the burning oil heats up above 350 °C (Speight, 2014). Regardless of the exact mechanisms, the results demonstrate that pyrogenic PAHs are created during the in-situ burning of crude oils and are taken up by their burned residues.

Overall, our results show that *n*-alkanes, isoprenoids and petrogenic PAHs all followed the diffusion-limited vaporization order. This result was observed for both DUC (with 5 mm and 20 mm initial thickness) and Grane. Correspondence to this vaporization order therefore seems to be independent of the initial chemical composition or physical appearance of the crude oil that was burned. As such, these results indicate that the diffusion-limited vaporization order is in general an applicable model for the in-situ burning of crude oil on water.

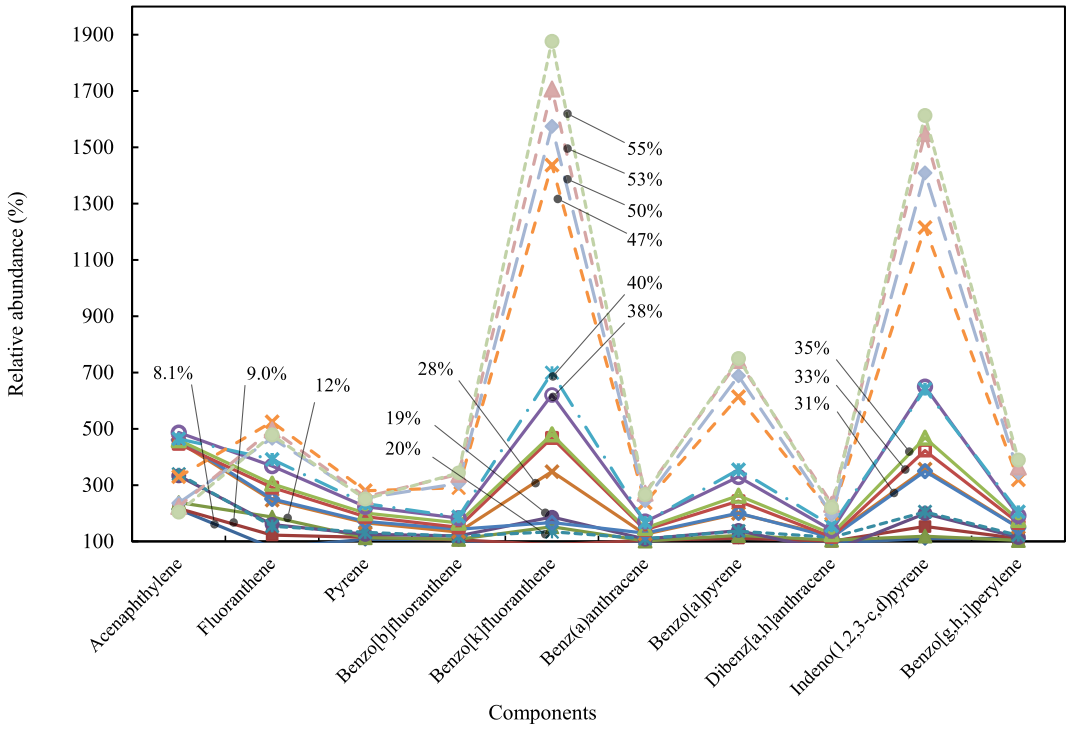

Fig. 6. Relative abundance of pyrogenic PAHs in burned 5 mm DUC residues as a function of the burning efficiency. The components are sorted in order of increasing retention time. The lighter and more volatile components participated in the fire earlier and were depleted faster from the burning crude oil than the heavier and less volatile components.

4. Conclusion

Three series (5 mm DUC, 20 mm DUC and 5 mm Grane) of small scale in-situ burning experiments were conducted to obtain a set of burned residues with a range of burning efficiencies (8.1%–69%). The burning efficiencies (with 10% intervals) were obtained by manually extinguishing the experiments at predetermined burning times, which were based on the burning rate of each crude oil. The results showed that the burning time was a reliable parameter to predict the burning efficiency, as the burning efficiencies from duplicate experiments were within an error margin of 1.4–11%. With increasing burning efficiency, the density and viscosity of the crude oils increased, which corresponds well with a vaporization order of the components in order of decreasing volatility.

Chemical analysis of the burned residues shows that the chemical composition of a burning crude oil and of the components evaporating from the oil changed constantly as the burning progressed. The depletion rate of *n*-alkanes, isoprenoids and petrogenic PAHs generally decreased with increasing molecular mass of the components. Furthermore, the higher the molecular mass of a component, the later it started to evaporate and participate in the fire. These results were independent of the initial chemical composition of the fresh crude oil or its physical appearance. Based on the results, it is clear that the diffusion-limited vaporization model best describes the vaporization order of burning crude oil on water. This conclusion means that as a crude oil burns, the energy required to maintain an evaporation rate that can sustain the fire constantly increases as the burning progresses. The practical implication of this conclusion is that the larger an in-situ burn is, and thus the more heat it produces, the longer the fire can be sustained and thus the higher the burning efficiency will be. For in-situ burning operations, the burning efficiency can then be governed through the size of the fire, irrespective of the chemical or physical properties of the spilled oil. Predicting the burning efficiency of in-situ burning a crude oil on water can thus be turned into a question of the heat balance during the fire, rather than the properties of the crude oil that is burned. A quantification of this heat balance will be required in order to be able to fully predict the burning efficiency of crude oil burning on water.

Pyrogenic PAHs were demonstrated to be produced during the in-situ burns, resulting in increased quantities of these PAHs in the burned residues. The highest increases were observed for benzo[k]fluoranthene (1876%, 2142% and 9108%), benzo[a]pyrene (750%, 974% and 482%) and indeno(1,2,3-c,d)pyrene (1613%, 2507% and 680%) in 5 mm DUC, 20 mm DUC and 5 mm Grane residues, respectively. Overall, the results highlight which pyrogenic PAHs are to be expected to form in large quantities during an in-situ burn and even provide a quantitative measure of their increase in abundance. Such information can be helpful for assessing the environmental impact that a burned crude oil residue may have when applying in-situ burning as oil spill response method.

Credit author statement

Laurens van Gelderen: Conceptualization, Methodology, Investigation, Writing – Original Draft, Visualization. Kristoffer Gulmark Poulsen: Formal analysis, Investigation, Writing – Original Draft, Jan H. Christensen: Methodology, Resources, Writing – Review & Editing, Supervision, Grunde Jomaas: Methodology, Resources, Writing – Review & Editing, Supervision, Funding acquisition.

Declaration of competing interest

The authors declare that they have no known competing financial interests or personal relationships that could have appeared to influence the work reported in this paper.

Acknowledgements

The authors would like to thank the Danish Council for Independent Research for funding the project (Grant DFF – 1335-00282). COWIfonden funded the construction of the Crude Oil Flammability Apparatus (project A-117.26) and Maersk Oil provided the crude oils that were used in this study. None of the sponsors have been involved in the results and conclusions of this paper.

Appendix A. Supplementary data

Supplementary data to this article can be found online at https://doi.org/10.1016/j.chemosphere.2021.131563.

References

Allen, A.A., 1990. Contained controlled burning of spilled oil during the Exxon Valdez oil spill. Proceedings of the Thirteenth Arctic and Marine Oilspill Program (AMOP) Technical Seminar. Environment Canada, pp. 305–313.

Allen, A.A., Jaeger, D., Mabile, N.J., Costanzo, D., 2011. The use of controlled burning during the gulf of Mexico deepwater Horizon MC-252 oil spill response. International Oil Spill Conference Proceedings. IOSC, pp. 1–13. https://doi.org/10.7901/2169-3358-2011-1-194.

Arai, M., Saito, K., Altenkirch, R.A., 1990. A study of boilover in liquid pool fires supported on water part I: effects of a water sublayer on pool fires. Combust. Sci. Technol. 71, 25–40. https://doi.org/10.1080/00102209008951622.

Bradford, M.L., Thodos, G., 1967. Latent heats of vaporization hydrocarbons. J. Chem. Eng. Data 12, 373–376. https://doi.org/10.1021/je60034a022.

Brogaard, N.L., Sørensen, M.X., Fritt-Rasmussen, J., Rangwala, A.S., Jomaas, G., 2014. A new experimental rig for oil burning on water - results for crude and pure oils. 11th International Symposium for Fire Safety Science. IAFSS, pp. 1481–1494.

Buist, I., Trudel, K., Morrison, J., Aurand, D., 1997. Laboratory studies of the properties of in-situ burn residues. International Oil Spill Conference Proceedings. IOSC, pp. 149–156. https://doi.org/10.7901/2169-3358-1997-1-149.

Buist, I., McCourt, J., Potter, S., Ross, S., Trudel, K., 1999. *In situ* burning. Pure Appl. Chem. 71, 43–65. https://doi.org/10.1351/pac199971010043.

Buist, I.A., Potter, S.G., Trudel, B.K., Shelnutt, S.R., Walker, A.H., Scholz, D.K., Brandvik, P.J., Fritt-Rasmussen, J., Allen, A.A., Smith, P., 2013. Arctic Response Technology. In: Situ Burning in Ice-Affected Waters: State of Knowledge Report, p. 293.

Carmichael, L.T., Berry, V.M., Sage, B.H., 1964. Viscosity of hydrocarbons. Propane. J. Chem. Eng. Data 9, 411–415. https://doi.org/10.1021/je60040a009.

CEN/TR 15522-2, 2012. Oil Spill Identification - Waterborne Petroleum and Petroleum Products - Part 2: Analytical Methodology and Interpretation of Results Based on GC-FID and GC-MS Low Resolution Analyses. European Committee for Standardization, Brussels, p. 142.

Chickos, J.S., Hanshaw, W., 2004. Vapor pressures and vaporization enthalpies of the n-alkanes from C_{21} to C_{30} at T = 298.15 K by correlation gas chromatography. J. Chem. Eng. Data 49, 77–85. https://doi.org/10.1021/je0301747.

Constantinidis, P., Schmitt, H.C., Fischer, I., Yan, B., Rijs, A.M., 2015. Formation of polycyclic aromatic hydrocarbons from bimolecular reactions of phenyl radicals at high temperatures. Phys. Chem. Chem. Phys. 17, 29064–29071. https://doi.org/10.1039/c5cp05354d.

Egloff, G., Sherman, J., Dull, R.B., 1940. Boiling point relationships among aliphatic hydrocarbons. J. Phys. Chem. 44, 730–745. https://doi.org/10.1021/j150402a006.

Fingas, M., 2011. An overview of in-situ burning. In: Fingas, M. (Ed.), Oil Spill Science and Technology. Gulf Professional Publishing, Oxford, pp. 737–903. https://doi.org/10.1016/B978-1-85617-943-0.10023-1.

Fingas, M.F., Li, K., Campagna, P.R., Turpin, R.D., Ackerman, F., Bissonnette, M.C., Lambert, P., Getty, S.J., Trespalacios, M.J., Belanger, J., Tennyson, E.J., 1994. Emissions from in situ oil fires. Situ Burning Oil Spill Workshop Proceedings. National Institute of Standards and Technology and Minerals Management Service, pp. 39–46.

Fritt-Rasmussen, J., Brandvik, P.J., Villumsen, A., Stenby, E.H., 2012. Comparing ignitability for in situ burning of oil spills for an asphaltenic, a waxy and a light crude oil as a function of weathering conditions under arctic conditions. Cold Reg. Sci. Technol. 72, 1–6. https://doi.org/10.1016/j.coldregions.2011.12.001.

Fritt-Rasmussen, J., Ascanius, B.E., Brandvik, P.J., Villumsen, A., Stenby, E.H., 2013. Composition of in situ burn residue as a function of weathering conditions. Mar. Pollut. Bull. 67, 75–81. https://doi.org/10.1016/j.marpolbul.2012.11.034.

Fritt-Rasmussen, J., Wegeberg, S., Gustavson, K., 2015. Review on burn residues from in situ burning of oil spills in relation to arctic waters. Water Air Soil Pollut. 226, 329. https://doi.org/10.1007/s11270-015-2593-1.

Gallotta, F.D.C., Christensen, J.H., 2012. Source identification of petroleum hydrocarbons in soil and sediments from Iguaçu River Watershed, Paraná, Brazil using the CHEMSIC method (CHEMometric analysis of Selected Ion Chromatograms). J. Chromatogr. A 1235, 149–158. https://doi.org/10.1016/j.chroma.2012.02.041.

Garo, J.P., Vantelon, J.P., Fernandez-Pello, A.C., 1994. Boilover burning of oil spilled on water. Symp. (Int.) Combust. 25, 1481–1488. https://doi.org/10.1016/S0082-0784(06)80792-7.

Garo, J.P., Vantelon, J.P., Gandhi, S., Torero, J.L., 1999. Determination of the thermal efficiency of pre-boilover burning of a slick of oil on water. Spill Sci. Technol. Bull. 5, 141–151. https://doi.org/10.1016/S1353-2561(98)00049-8.

John, G.F., Han, Y., Clement, T.P., 2018. Fate of hopane biomarkers during in-situ burning of crude oil — a laboratory-scale study. Mar. Pollut. Bull. 133, 756–761. https://doi.org/10.1016/j.marpolbul.2018.06.036.

Korsten, H., 2001. Viscosity of liquid hydrocarbons and their mixtures. AIChE J. 47, 453–462. https://doi.org/10.1002/aic.690470222.

Law, C.K., 1978. Internal boiling and superheating in vaporizing multicomponent droplets. AIChE J. 24, 626–632. https://doi.org/10.1002/aic.690240410.

Law, C.K., 2006. Combustion Physics. Cambridge University Press, New York.

Maersk Oil, 2005. DUC Crude Oil. Maersk Olie Og Gas AS.. Retrieved 1st of January, 2017, from. www.maerskoil.com/about-us/Documents/Sales/DUCassay.xls

Nolan, D.P., 2011. 4 - physical properties of hydrocarbons. Handbook of Fire and Explosion Protection Engineering Principles, second ed. William Andrew Publishing, Oxford, pp. 33–48. https://doi.org/10.1016/B978-1-4377-7857-1.00004-5.

Petty, S.E., 1983. Combustion of crude oil on water. Fire Saf. J. 5, 123–134. https://doi.org/10.1016/0379-7112(83)90005-X.

Piacente, V., Fontana, D., Scardala, P., 1994. Enthalpies of vaporization of a homologous series of n-alkanes determined from vapor pressure measurements. J. Chem. Eng. Data 39, 231–237. https://doi.org/10.1021/je00014a009.

Potter, S., Buist, I., 2008. In-situ burning for oil spills in arctic waters: state-of-the-art and future research needs. In: Davidson, W.F., Lee, K., Cogswell, A. (Eds.), Oil Spill Response: A Global Perspective. Springer Netherlands, pp. 23–39. https://doi.org/10.1007/978-1-4020-8565-9_5.

Prosen, E.J., Rossini, F.D., 1945. Heats of combustion and formation of the paraffin hydrocarbons at 25 C. J. Res. Natl. Inst. Stan. 34, 263–269.

Růžička, K., Majer, V., 1994. Simultaneous treatment of vapor pressures and related thermal data between the triple and normal boiling temperatures for n-alkanes C_5–C_{20}. J. Phys. Chem. Ref. Data 23, 1–39. https://doi.org/10.1063/1.555942.

Seaton, W.H., Keith Harrison, B., 1990. A new general method for estimation of heats of combustion for hazard evaluation. J. Loss Prev. Process. Ind. 3, 311–320. https://doi.org/10.1016/0950-4230(90)80025-6.

Speight, J.G., 2014. Refining Chemistry. The Chemistry and Technology of Petroleum. Chapman and Hall/CRC, ProQuest Ebook Central, pp. 433–458.

Statoil, 2017. Grane Blend. Statoil.. Retrieved 10th of August, 2017, from. https://www.statoil.com/content/dam/statoil/documents/crude-oil-assays/GRANE-BLEND-2017-01.xls

Stout, S.A., Payne, J.R., 2016. Chemical composition of floating and sunken in-situ burn residues from the Deepwater Horizon oil spill. Mar. Pollut. Bull. 108, 186–202. https://doi.org/10.1016/j.marpolbul.2016.04.031.

Van Gelderen, L., Jomaas, G., 2018. Experimental procedure for laboratory studies of in situ burning : Flammability and burning efficiency of crude oil. JoVE, e57307. https://doi.org/10.3791/57307.

Van Gelderen, L., Brogaard, N.L., Sørensen, M.X., Fritt-Rasmussen, J., Rangwala, A.S., Jomaas, G., 2015. Importance of the slick thickness for effective in-situ burning of crude oil. Fire Saf. J. 78, 1–9. https://doi.org/10.1016/j.firesaf.2015.07.005.

Van Gelderen, L., Malmquist, L.M.V., Jomaas, G., 2017. Vaporization order and burning efficiency of crude oils during in-situ burning on water. Fuel 191, 528–537. https://doi.org/10.1016/j.fuel.2016.11.109.

Vetere, A., 1979. New correlations for predicting vaporization enthalpies of pure compounds. Chem. Eng. J. 17, 157–162. https://doi.org/10.1016/0300-9467(79)85008-X.

Wang, C.H., Liu, X.Q., Law, C.K., 1984. Combustion and microexplosion of freely falling multicomponent droplets. Combust. Flame 56, 175–197. https://doi.org/10.1016/0010-2180(84)90036-1.

Wang, Z., Fingas, M., Shu, Y.Y., Sigouin, L., Landriault, M., Lambert, P., Turpin, R., Campagna, P., Mullin, J., 1999. Quantitative characterization of PAHs in burn residue and soot samples and differentiation of pyrogenic PAHs from petrogenic PAHs—The 1994 mobile burn study. Environ. Sci. Technol. 33, 3100–3109. https://doi.org/10.1021/es990031y.

Yaws, C.L., 2015. Chapter 1 - physical properties – organic compounds. The Yaws Handbook of Physical Properties for Hydrocarbons and Chemicals, second ed. Gulf Professional Publishing, Boston, pp. 1–683. https://doi.org/10.1016/B978-0-12-800834-8.00001-3.